Running title: Category-specific distal connections

Manuscript in press at *Cortex*

Overlapping but distinct: distal connectivity dissociates hand and tool processing networks

Amaral, L.[1,2], Bergström, F. [1,2,¥*], & Almeida, J.[1,2,¥*]

1. Proaction Laboratory, Faculty of Psychology and Educational Sciences, University of Coimbra. Portugal

2. CINEICC, Faculty of Psychology and Educational Sciences, University of Coimbra. Portugal

*Correspondence should be sent to:

Jorge Almeida, Proaction Laboratory, Faculty of Psychology and Educational Sciences, University of Coimbra. Rua do Colégio Novo 3001-802 Coimbra, Portugal.

jorgecbalmeida@gmail.com

Fredrik Bergström, Proaction Laboratory, Faculty of Psychology and Educational Sciences, University of Coimbra. Rua do Colégio Novo 3001-802 Coimbra, Portugal.

f.bergstroem@gmail.com

¥ These authors contributed equally to this paper.

Acknowledgments

This work was supported by the Foundation for Science and Technology of Portugal and Programa COMPETE grant (PTDC/MHC-PCN/6805/2014) to JA. LA is supported by Foundation for Science and Technology of Portugal individual PhD grant (SFRH/BD/114811/2016). FB is supported by Foundation for Science and Technology of Portugal individual researcher grant (CEECIND/03661/2017). JA is supported by an European Research Council Starting Grant ("ContentMAP" - 802553). We thank Philipp Seidel and Jon Walbrin for their help in data analysis.

Abstract

The processes and organizational principles of information involved in object recognition have been a subject of intense debate. These research efforts led to the understanding that local computations and feedforward/feedback connections are essential to our representations and their organization. Recent data, however, has demonstrated that distal computations also play a role in how information is locally processed. Here we focus on how long-range connectivity and local functional organization of information are related, by exploring regions that show overlapping category-preferences for two categories and testing whether their connections are related with distal representations in a category-specific way. We used an approach that relates functional connectivity with distal areas to local voxel-wise category-preferences. Specifically, we focused on two areas that show an overlap in category-preferences for tools and hands – the inferior parietal lobule/anterior intraparietal sulcus (IPL/aIPS) and the posterior middle temporal gyrus/lateral occipital temporal cortex (pMTG/LOTC) – and how connectivity from these two areas relate to voxel-wise category-preferences in two ventral temporal regions dedicated to the processing of tools and hands separately – the left medial fusiform gyrus and the fusiform body area respectively – as well as across the brain. We show that the functional connections of the two overlap areas correlate with categorical preferences for each category independently. These results show that regions that process both tools and hands maintain object topography in a category-specific way. This potentially allows for a category-specific flow of information that is pertinent to computing object representations.

Keywords: tools; hands; distal connectivity; representation; functional organization; fMRI

Introduction

The human brain has the ability to immediately recognize familiar objects on sight, and it does so while managing many different kinds of information (e.g., shape, texture, function). However, the cortical organization of this information, and the neural computations supporting these processes are still under debate (Grill-Spector & Malach, 2004). Here we will take on a recent proposal on how object information is represented in the brain, which proposes that local processing is influenced, in part, by processing happening distally within the neural network dedicated to the processing of the target category. We will focus on the processing of tool and hand stimuli to further explore how representations are modulated distally.

Early neuroimaging studies showed that different object categories engage different sets of cortical areas (e.g., faces; Kanwisher et al., 1997; places/scenes; e.g., Epstein & Kanwisher, 1998; tools; e.g., Almeida et al., 2013; Chao & Martin, 2000; Mahon et al., 2007; bodies; e.g., Downing et al., 2001; and hands; e.g., Bracci et al., 2012, 2016). However, current theories differ in their understanding of what drives this object topography – whether it is the distributed representation of object features (Haxby et al., 2001; Konkle & Caramazza, 2013), the typical visual field location of different categories (Levy et al., 2001); or domain-specific constraints (e.g., Caramazza & Shelton, 1998; Kriegeskorte et al., 2008; Mahon & Caramazza, 2011, for a review Grill-Spector & Malach, 2004). Importantly, most share the view that neural specificity and conceptual representations arise from local computations, feedforward connectivity from early visual regions, and attentional and/or perceptual feedback connections (e.g., Bar et al., 2006; Buffalo et al., 2010; Kreiman et al., 2010).

A conceptually different approach for thinking about object topography is that local representations also depend on connections from distal regions that share categorical

preference. In this view, local representations do depend on local computations, feedforward and feedback connections, as described before, but also, and importantly, on connections from distal regions that share categorical preference (and that pertain to the same level of representation). That is, local representations are constrained by connectivity with other brain areas at the same level in the visual processing hierarchy (Almeida et al., 2013; Chen et al., 2017; Garcea et al., 2019; Hutchison et al., 2014; Hutchison & Gallivan, 2018; Lee et al., 2019; Mahon & Caramazza, 2009, 2011; Walbrin & Almeida, 2021). In support of this view, representations in a tool-preferring region (the left medial fusiform gyrus; mFUG) within the ventral temporal cortex (VTC) are causally dependent on computations in remote but functionally connected tool-preferring regions within parietal cortex (the Inferior Parietal Lobule; IPL; Lee et al., 2019; see also Ruttorf et al., 2019; Garcea et al., 2019). Moreover, functional and structural connectivity from distant regions correlate with categorical preferences in VTC in a category-specific way (e.g., functional connectivity between tool-preferring IPL and VTC correlated with tool preferences but not place, animal, or face preferences in the VTC; Chen et al., 2017; see also Pessoa et al., 2006; Saygin et al., 2016; Zhang et al., 2009).

Most of the work that tried to dissect the relationship between local computations and distal connectivity has been done over distal regions that respond preferentially to one specific object category (out of those being tested; e.g., tools in an experimental design that includes stimuli from the category of animals, faces or places; Chen et al., 2017). A stronger case of this hypothesis could be made by testing distal regions that respond preferentially to more than one category of those tested. For instance, if a region responds equally to two categories as revealed by BOLD signal, do its connections relate to object topography elsewhere in a category-specific way – i.e., do its connections disentangling the processing of the two categories? According to the hypothesis proposed

above, the functional connections of these regions should nevertheless correlate with response preferences in regions that are distally located in a category-specific manner, and should do so independently for each one of the categories, thus maintaining object topography irrespectively of the overlap in BOLD signal responses for the two categories.

Here we will focus on the categories of tools and hands, because tools and hands are functionally related (Almeida et al., 2018), and because some of the regions that these stimuli preferentially engage are shared (e.g., Almeida et al., 2013; Bracci et al., 2012, 2016; Bracci & Peelen, 2013; Chao & Martin, 2000; Mahon et al., 2007; Peeters et al., 2013). On the one side, tool stimuli (when compared to items from other categories such as animals or faces) lead to heightened activation bilaterally in superior parietal cortex, dorsal occipital cortex, and the medial fusiform gyrus, and within left inferior parietal regions, the anterior intraparietal sulcus (aIPS), ventral premotor cortex, and posterior middle temporal areas (e.g., Almeida et al., 2013, 2017; Binkofski et al., 1999; Binkofski et al., 1998; Chao et al., 1999; Chao & Martin, 2000; Chen et al., 2017; Freud et al., 2017; Kristensen et al., 2016; Mahon et al., 2013, 2007; Noppeney et al., 2006; Peeters et al., 2013). On the other side, hand stimuli (when compared to other categories of interest such as animals) lead to stronger responses within lateral fusiform gyrus bilaterally, lateral occipital temporal cortex (stronger on the left), in inferior and superior parietal regions, and in premotor, somatosensory, and motor regions (e.g., Bracci et al., 2010, 2012, 2016; Bracci & Peelen, 2013; Grosbras & Paus, 2006; Meier et al., 2008; Peeters et al., 2013).

Importantly, in a series of studies Bracci and Colleagues have demonstrated that tool and hand stimuli concurrently engage two regions - the left IPL and left posterior middle temporal gyrus/lateral occipital temporal cortex (pMTG/LOTC) (Bracci et al., 2012, 2016; Bracci & Peelen, 2013; Peeters et al., 2013). Given this response overlap between tool and hand stimuli within the left IPL and the left pMTG/LOTC, we predict

that functional connectivity from each of these overlap regions (i.e., left IPL or left pMTG/LOTC) to distal regions (e.g., regions within the VTC) should be correlated with voxel-wise response preferences within those distal regions. This should be so in a category-specific way and thus should be able to disentangle the tool and hand networks despite the BOLD response overlap for tools and hands within left IPL and left pMTG/LOTC.

We answer this question by focusing on the two overlap sites (IPL and pMTG/LOTC), and examine how multivoxel categorical preferences for tools and hands in particular areas of the tool and hand networks, and across the brain, correlate with functional connectivity emerging from these overlapping areas (see Figure 1A). We predict that voxel-wise tool-preferences but not hand-preferences in the medial aspects of the fusiform gyrus (the mFUG; an area that is part of the tool network; Chao & Martin, 2000; Mahon et al., 2007) will correlate strongly with functional connectivity computed from each overlap region (i.e., IPL or pMTG/LOTC) to the voxels within the medial fusiform, whereas the inverse will be true in more lateral aspects of the fusiform (i.e., the Fusiform Body Area - FBA; an area that shows preferences for body parts and hands; Downing et al., 2001). We will then inspect the whole brain for similar category-specific distal modulations by using a searchlight approach, and expect to observe different distal relationships for tools and hands emerging from the two overlap areas.

Figure 1. Experimental procedures and analysis pipeline.

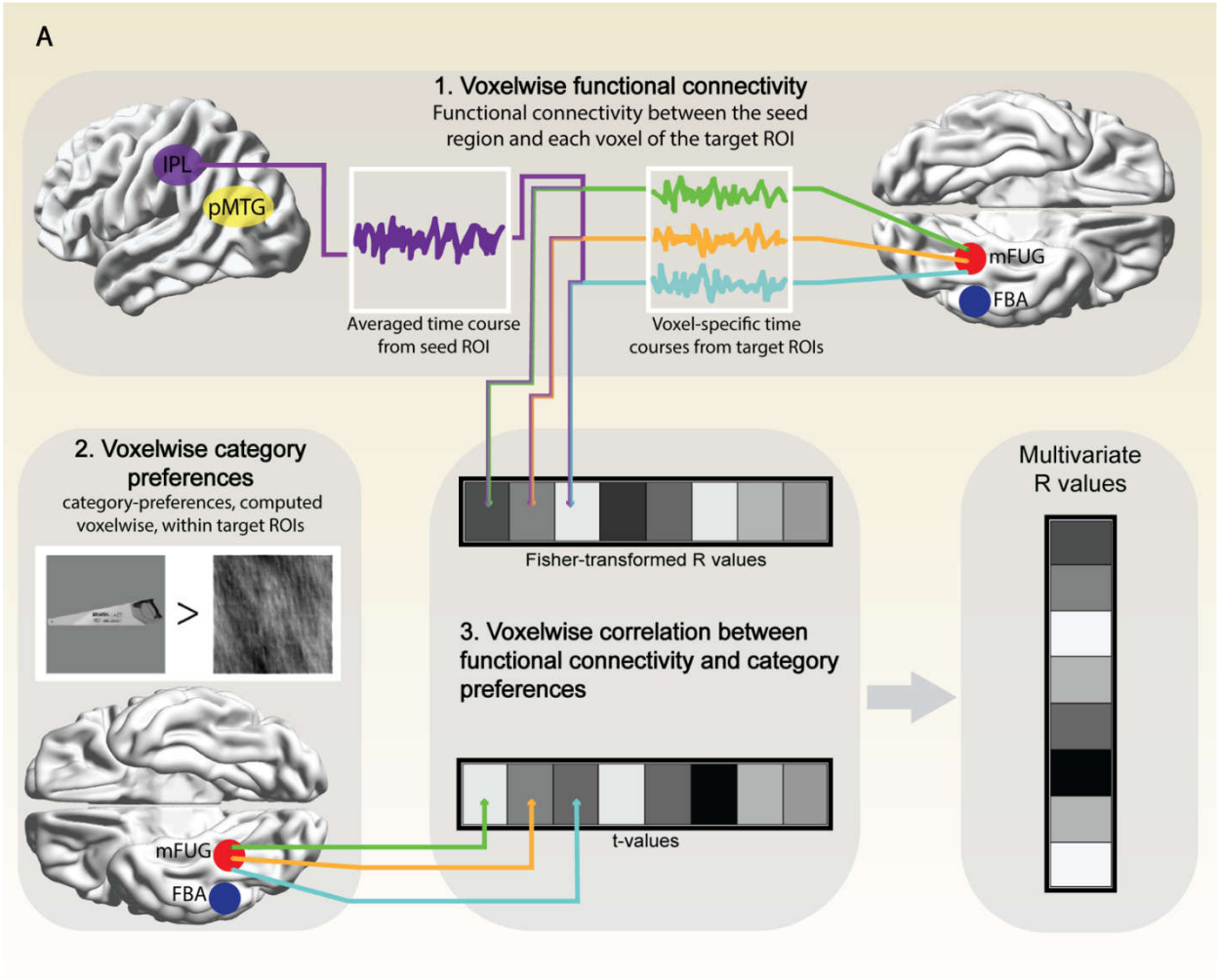

(*) 12 images * 500ms = 6s

Experimental procedures and analysis pipeline. (**A**) Schematic workflow of analysis. (1) an average seed time-series (e.g., IPL/aIPS) is correlated with the time-series of each voxel in a target ROI (e.g., mFUG) to produce a vector of Fischer transformed r-values. (2) a univariate contrast (e.g., tools > all scrambled) in the same target ROI is used to produce a vector of category-preference (t-values). (3) the Fischer transformed r-values are correlated with the t-values within the target ROI to produce multivariate r-values. (**B**) Blocked fMRI design with 12 images (each 500 ms) per block (each 6 s) of tools, hands, animals, places, and phase-scrambled images, with 16 s fixation between blocks (**C**) The VTC regions of interest used during the analysis (FBA in blue and mFUG in red). The regions were defined around peak coordinates obtained in the literature.

Materials and Methods

The conditions of our ethics approval do not permit public archiving of anonymized study data. Readers seeking access to the data should contact the corresponding author through email. Full access to the data will be granted on request without conditions. Stimuli are available at https://osf.io/2j8ym/. No part of the study procedures and analysis was pre-registered prior to the research being conducted. We report how we determined sample size, all data exclusions (if any), all inclusion/exclusion criteria, whether inclusion/exclusion criteria were established prior to data analysis, all manipulations, and all measures in the study.

Participants

We recruited sixteen participants (M = 21 years, SD = 4.7, 12 females) from the subject pool of the Faculty of Psychology and Educational Sciences of the University of Coimbra following previous studies (e.g., Mahon et al, 2013). All participants had normal

or corrected to normal vision, were right-handed, gave written informed consent, and received course credits for their participation. The study adhered to the Declaration of Helsinki and was approved by the Ethical Committee of the Faculty of Psychology and Educational Sciences at the University of Coimbra. Due to excessive head motion, we excluded data from all runs for one participant. Thus, 15 participants were used for statistical analyses.

Stimuli and procedure

The study consisted of a category-preference experiment (6 runs with a total of 546 volumes per participant) and a tool/hand experiment (5 runs; participants also went through another session of this experiment, but that data was not used herein) where task-related BOLD signal was regressed out in order to calculate functional connectivity measures unrelated to the task. Stimulus delivery and response collection was controlled using "A Simple Framework" (Schwarzbach, 2011) based on the Psychophysics Toolbox on Matlab R2014a (The MathWorks Inc., Natick, MA, USA). Stimuli (Figure 1b) were presented on an Avotec projector with a refresh rate of 60 Hz, and viewed by the participants through a mirror attached to the head coil inside the bore of the MR scanner.

In the category-preference experiment participants passively viewed grey-scaled images (400 x 400 pixel-size) of tools, hands, animals, famous places, and phase-scrambled versions of each category (adapted from Fintzi & Mahon, 2014; see also Almeida et al., 2017; Lee et al., 2019). Each category was pseudo-randomly presented block-wise (with 12 consecutive images presented for 500 ms each per block) twice per run. Each phase-scrambled object category was presented once per run, each block was separated by 6 s fixation periods, and each run began and ended with a 16 s fixation period.

In the tool/hand experiment we used a mixed design with six 54 s blocks, 8 s inter-block-intervals, and each block contained 18 randomly mixed trials with 1.5 s stimulus and 1.5 s fixation. There were two blocks of grey-scaled (8 power and 8 precision) tool images, two blocks of grey-scaled (8 power and 8 precision) grasp videos filmed from a first-person viewpoint, and two blocks of grasp videos filmed from a third-person viewpoint. Additionally, each block contained two "catch" trials, which were either tool chimeras (i.e., a combination of two tools) in the tool-image block, or a non-grasping movement (e.g., rotating the hand while maintaining an open palm) in the grasp-video blocks. Participants were instructed to pay attention to the presented stimuli and press a button whenever they detected a catch trial. Critically, however, the experimental design of this tool/hand task was regressed out (see below) and the residuals were used to compute functional connectivity (e.g., Almeida et al., 2013).

For all experiments, we used an eye tracker to (subjectively) monitor the individual's attention (and wakefulness) during the task.

MRI acquisition

We collected MRI data with a 3T MAGNETOM Trio whole body MR scanner (Siemens Healthineers, Erlangen, Germany) with a 32-channel receive-only head coil across two sessions (one structural run, six runs for the category-preference experiment and five runs for the tool/hand experiment). We acquired structural MRI data using a T1-weighted magnetization prepared rapid gradient echo (MPRAGE) sequence (repetition time (TR) = 1900 ms, echo time (TE) = 2.32 ms, slice thickness = 0.9 mm, flip angle = 9 degrees, field of view (FoV) = 256 x 256, matrix size = 256 x 256, bandwidth (BW) = 200 Hz/px, GRAPPA acceleration factor 2). Functional MRI (fMRI) data were acquired using a T2*-weighted gradient echo planar imaging (EPI) sequence (TR = 2000 ms, TE = 22 ms, slice thickness = 2.3, FoV = 256 x 256, matrix size = 96 x 96, flip angle = 90

degrees, BW = 1578 Hz/px, GRAPPA acceleration factor 3). Each image volume consisted of 40 contiguous transverse slices recorded in interleaved slice order oriented parallel to the line connecting the anterior commissure to the posterior commissure covering the whole brain.

fMRI data Preprocessing

We used SPM12 (Welcome Trust Centre for Neuroimaging, London, UK), run in Matlab R2018b (Mathworks, Inc., Sherborn, MA, USA), for processing and analysis of structural and functional data. The structural and functional images were reoriented to approximate MNI space with SPM12 after slice-time correction. During preprocessing, the functional data were slice-time corrected to the first slice using a Fourier phase-shift interpolation method, corrected for head motion to the first volume of the first session using 7^{th} degree b-spline interpolation. Structural images were coregistered to the first functional images. Functional data were normalized to MNI anatomical space using a 12-parameter affine transformation model in DARTEL (Ashburner, 2007) and down-sampled to 3 mm^3 voxel size prior to applying an 8 mm (for ROIs definition) and 6 mm (for category-preferences and functional connectivity analyses) FWHM Gaussian filter.

Statistical analysis of fMRI data

In order to preserve independence between voxel selection and testing (Kriegeskorte et al., 2009), each participant's data were split into three datasets: i) the first two runs from the category-preference experiment were used to define ROIs, ii) the remaining four runs were used to measure category-preferences, and iii) the five runs from the tool/hand experiment were used to compute functional connectivity.

Moreover, we followed two main analytical pipelines. In the first (Figure 1a) we used specific target ROIs within VTC that are preferentially engaged by either tools (the mFUG) or hands (the FBA) from which we extracted categorical preferences (t-values)

for each voxel in the ROI, and correlated these preferences with functional connectivity data from our seed ROIs. In the second analysis, we computed categorical preferences across the brain (for each voxel within the sphere visited) using a searchlight analysis and correlated these with functional connectivity from our seed ROIs.

Univariate analysis. For each participant and for each experiment (category-preference and tool/hand experiment), a fixed effects analysis was performed independently by setting up a General Linear Model (GLM) including the following regressors of interest for the category-preference experiment: animals, hands, places, tools and phase-scrambled pictures. For the tool/hand experiment, the following nuisance regressors were used: grasp (first person perspective), grasp (third person perspective), tools, grasp catch trials, and tool catch trials. We used these regressors to remove task-based signal. All regressors of interest were convolved with a canonical hemodynamic response function (first order expansion) to create the design matrix. The motion correction parameters were used as a nuisance regressor to covary out signal correlated with head motion. Model estimations for each participant were used in a second-level random-effects analysis to account for inter-individual variability.

Seed definition. A conjunction contrast (tools > animals ∩ hands > places) was used to define left IPL (average peak MNI coordinates: -34 ± 4.8, -47 ± 5.04, 49 ± 3.96; see Supplementary Figure 1 and Supplementary Table 1) and left pMTG/LOTC (average peak MNI coordinates: -44 ± 4.83, -69 ± 2.97, -1 ± 3.96) as seed regions for the functional connectivity. Because the left IPL seed encompassed also regions within the aIPS (see supplementary Figure 1 and supplementary Table 1), we will refer to it as the IPL/aIPS seed. We created a 10 mm sphere around each participant's peak voxel, within which the 100 voxels with highest t-value were selected. One participant only performed 4 runs from the category-preference experiment, so we did not use any data from this participant

to define the ROIs. For this particular participant, we created the spheres around the group peak voxels.

Target ROI definition. Two target ROIs per hemisphere were selected: the tool- and body-preferring areas within the fusiform gyrus (Figure 1c). We used both hemispheres as the category preferences for tools and hands in these VTC regions are bilateral. We defined spheres with 9 mm radius centered on peak-voxel coordinates reported in previous studies (tool-preferring mFUG – left MNI coordinates: [-24 -53 -9], right: [24 -42 -16] – Mahon et al., 2007; body-preferring FBA – left MNI coordinates: [-40 -48 -22], right: [40 -48 -22] – Vocks et al., 2010). Voxels located in the cerebellum were removed from the spherical ROIs.

Measuring category-preferences. Category-preferences for each voxel within the target ROIs or the searchlight kernel were computed by contrasting each target category (tools or hands) against all scrambled categories (e.g., tools > all scrambled). Contrast weighted t-values of each contrast were thus obtained for each voxel of the target ROI or the searchlight sphere.

Functional connectivity analysis. All functional connectivity was computed from the data collected from the tool/hand experiment using the CONN Toolbox (Whitfield-Gabrieli & Nieto-Castanon, 2012). Time courses were extracted from the 5 runs and potential confounding effects were estimated and removed separately for each voxel and for each participant and run. Potential confounding effects used in CONN Toolbox that we included in our analysis were: noise components from white matter and cerebrospinal fluid, subject-motion parameters and main task effects. All these confounding effects were regressed out, and functional connectivity was computed over the residual time series, after covarying out the experimental design. Design-regressed task data has been extensively used in the past to calculate functional connectivity (e.g.,

Almeida et al., 2013; Norman-Haignere et al., 2012; Tran et al., 2018), and it has been shown that it effectively leads to similar functional connectivity estimates as when using resting scans (Fair, Schlaggar, Cohen, Miezin, Dosenbach et al., 2007). Functional connectivity was then computed between a seed ROI (averaging all time courses from each voxel) and each voxel in a target ROI. The resulting r-values were then Fisher transformed. Thus, each voxel in the target ROIs had two r-value scores – one for each seed ROI, corresponding to the functional connectivity of each voxel with each of the overall seed ROI – along with two t-values from the hand and tool category-preferences (as described above).

Analysis of the correlations between functional connectivity from the seed ROIs and category preferences distally

ROI Analysis. We computed the multivoxel linear correlation between the distribution of functional connectivity (with each seed region) and the category-preferences for each voxel in the target ROIs (for a similar approach see Chen et al., 2017). Specifically, and for each combination of target ROI, seed ROI, and categorical preference (tool-preferences or hand-preferences) separately, we correlated the category-preferences for the specific category in each voxel of the target ROI with the functional connectivity of those voxels with the selected seed region. That is, at each voxel in the target ROI we would have a contrast weighted t-value for the particular category preference being tested, and a fisher-transformed r-value from the functional connectivity analysis to the specific seed ROI being tested. These multivoxel values (*t*-values and r-values) were then linearly correlated as a proxy of modulation between the functional connections of a region and category-preferences in a distal region. Before computing this correlation, we also checked for heteroscedasticity of the variables (Table 1) using the Breusch-Pagan test (Kamarov, 2020). We rejected the null hypothesis that the

residuals are homoscedastic for tests showing a $p < .05$. For these cases (4 out 16), we calculated the Spearman's correlation instead of Pearson's. Consequently, we had a 2 (seed ROI: left IPL/aIPS, left pMTG/LOTC) * 2 (target ROI: mFUG, FBA) * 2 (category-preferences: tools, hands) * 2 (hemisphere of the target ROIs: left and right) factor design. The multivariate correlations between functional connectivity and category-preferences were therefore analyzed with a repeated measure ANOVA with these four factors. Specifically, we were interested in whether there was an interaction between the target ROIs and the category-preferences. Moreover, and as a control, we were interested in the interaction of these two main factors with the factors seed ROI and hemisphere.

Table 1.

Breusch-Pagan tests.

	Preferences (t-values)	
Functional connectivity (r-values)	**Hands**	**Tools**
IPL/aIPS - left FBA	.0125*	.4299
IPL/aIPS - right FBA	.6343	.8796
IPL/aIPS - left mFUG	.0015**	.9776
IPL/aIPS - right mFUG	.7067	.4378
pMTG/LOTC- left FBA	.0296*	.1752
pMTG/LOTC- right FBA	.8502	.5883
pMTG/LOTC- left mFUG	.0907	.3503
pMTG/LOTC - right mFUG	.5475	.0255*

*LOTC – lateral occipital temporal cortex; pMTG – posterior middle temporal gyrus; IPL – inferior parietal lobule; aIPS – anterior intraparietal sulcus; mFUG – middle fusiform Gyrus; FBA – fusiform body area; *p < .05; ** p < .01*

Searchlight analysis. We conducted a whole-brain searchlight analysis (e.g., Chen et al., 2017; Kriegeskorte et al., 2006) in order to relate functional connectivity to category-preferences. For each participant, we had two different whole-brain functional connectivity maps for each seed region (IPL/aIPS and pMTG/LOTC), and two whole-

brain category-preference t-maps for tools and hands. For every sphere (number of surrounding voxels = 50) in the searchlight, we extracted (i) contrast-weighted t-values for a given object-preference, (ii) Fisher transformed correlation coefficients (functional connectivity) from each seed region. These values were then correlated. The resulting Fisher transformed correlation coefficient was saved in each sphere's center voxel, which resulted in a whole-brain Fisher transformed r-value map. The searchlight procedure was performed 4 times for each participant (2 connectivity maps [IPL/aIPS and pMTG/LOTC seeds] * 2 category-preferences maps [tools and hands]). Finally, we created statistical group maps for all four conditions by performing two-tailed one-sample t-tests on the Fisher transformed correlation coefficients across participants. The resulting z-maps were corrected for multiple comparisons using threshold-free cluster-enhanced (TFCE; Smith & Nichols, 2009) Monte Carlo simulations with 10,000 iterations as implemented in CoSMoMVPA Toolbox (Oosterhof et al., 2016). Furthermore, to analyze differences between maps generated by hand- and tool-preferences, we only used voxels with $r > .45$ (corresponding to $p = .001$), and performed a one-tailed two-sample t-test to compare tools vs. hands for each seed region (IPL/aIPS and pMTG/LOTC). The resulting z-maps were corrected for multiple comparisons using TFCE Monte Carlo simulation with 10,000 iterations (Oosterhof et al., 2016).

Results

Relating functional connectivity from distal (IPL/aIPS and pMTG/LOTC) regions and local category-preferences in tool- or hand-preferring VTC regions. We used a 2 (seed ROI: left IPL/aIPS or left pMTG/LOTC) * 2 (target ROI: mFUG or FBA) * 2

(category-preference: tools or hands) * 2 (hemisphere of the target ROIs: left or right) factor repeated-measures ANOVA to analyze the Fisher transformed r-values from correlating category-preference contrast-weighted t-values and Fisher transformed functional connectivity r-values.

As predicted, there was a significant target ROI and category-preference interaction ($F(1,14) = 24.691$, $p < .0001$) such that the correlation between category-preferences and connectivity measures differs between the two target regions (mFUG and FBA) within the VTC (Figure 2). Post-hoc tests (Holm-Bonferroni corrected; Holm, 1978) revealed that the correlation between tool-preferences and functional connectivity (irrespective of the seed region) was higher than the correlation between hand-preferences and functional connectivity in mFUG ($t(14) = 4.73$, adjusted $p = .0006$). The reverse was true for FBA – the correlation between hand-preferences and functional connectivity was higher than the correlation between tool-preferences and functional connectivity ($t(14) = 2.26$, adjusted $p = .040$). There was no target ROI * category-preference * hemisphere interaction ($F(1,14) = 1.187$, $p = .294$), seed ROI * target ROI * category-preference interaction ($F(1,14) = .085$, $p = .775$), nor target ROI * category-preference * seed ROI * hemisphere interaction ($F(1,14) = 1.546$, $p = .234$). This shows that seed ROI and the

hemisphere of the target region are not leading to differential results in the correlation of functional connectivity and category-preferences in the target ROIs.

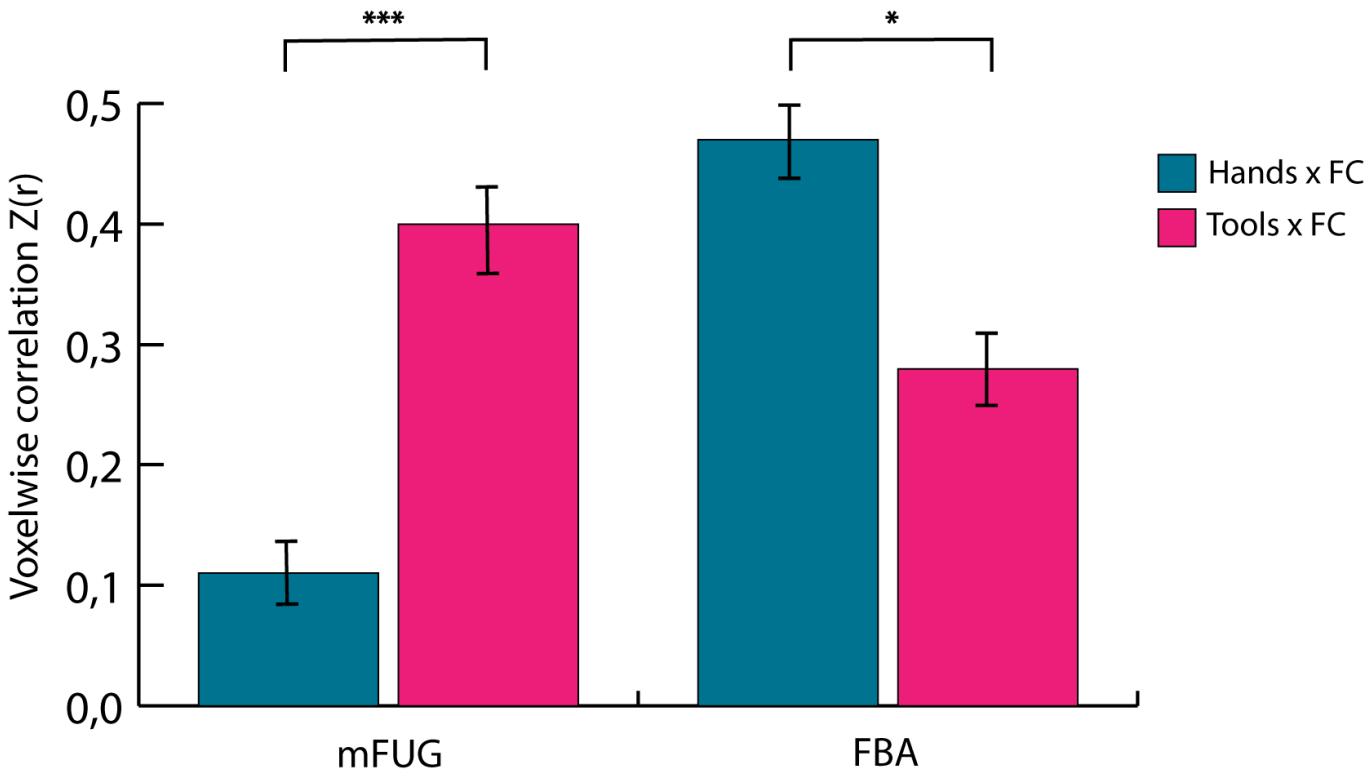

Figure 2. ROI results

ROI results. Voxelwise correlation between category-preferences (t-values) and functional connectivity (Fischer transformed r-values) within target regions of interest, demonstrating an interaction. All error bars reflect one standard error of the mean across participants. P-values are Holm-Bonferroni corrected for 2 tests (* = adjusted p value < .05; *** = adjusted p value < .001). (mFUG – medial Fusiform Gyrus; FBA – Fusiform Body Area; FC – Functional Connectivity)

In addition to the tests of interest, we obtained other significant effects. There was a main effect of category-preference ($F(1,14) = 7.085$, $p = .019$) such that correlations involving tool-preferences were greater than those involving hand-preferences. There was also a seed * target ROI interaction ($F(1,14) = 5.046$, $p = .041$). However, post-hoc tests only indicated a trend in the correlations between category-preferences and functional

connectivity over mFUG and FBA from the two seed ROIs. Correlations between category-preferences and functional connectivity over the mFUG were nominally higher from IPL/aIPS than pMTG/LOTC ($t(14) = 1.84$, $p = 0.087$), whereas correlations between category-preferences and functional connectivity over FBA were nominally higher from pMTG/LOTC than IPL/aIPS ($t(14) = 1.82$, $p = 0.091$). Finally, there was a target ROI * hemisphere interaction ($F(1,14) = 4.668$, $p = .049$), but post-hoc comparisons were not significantly different from 0. Accordingly, correlations between category-preferences and functional connectivity over mFUG were not different between hemispheres ($t(14) = 1.32$, $p = 0.207$), whereas correlations between category-preferences and functional connectivity over FBA were nominally higher in the left hemisphere ($t(14) = 1.95$, $p = 0.071$). No other main effects or interactions were significant (all $p < .869$).

Connectivity from IPL/aIPS and from pMTG/LOTC correlated with tool and hand preferences differ for different parts of the brain, constraining object topography across the brain. The searchlight analysis showed that connectivity from IPL/aIPS and pMTG/LOTC correlated with tool and hand preferences differentially across the brain (Table 2 and Figure 3; see also Supplementary Figure 2). On the one hand, functional connectivity from IPL/aIPS correlated with tool-preferences in the left mFUG, and functional connectivity from the left pMTG/LOTC correlated with tool-preferences in the mFUG (bilaterally), and in the left dorsal occipital cortex (including cuneus, precuneus, and partly superior parietal lobule). On the other hand, functional connectivity from the left IPL/aIPS correlated with hand-preferences in the left postcentral gyrus/somatosensory cortex, specifically in the hand area (Roux et al., 2018), and the left superior temporal sulcus (STS), and functional connectivity from the left pMTG/LOTC correlated with hand-preferences in right the STS extending inferiorly and posteriorly,

but not overlapping with the functionally defined right pMTG/LOTC (see Supplementary Figure 3).

Table 2.

MNI coordinates from the brain regions extracted during the searchlight analyses.

Seed ROI	Category-preference	Brain regions	MNI coordinates			Cluster size	Peak z-value
			x	y	z		
pMTG/LOTC	Tools	Left dorsal occipital cortex	-18	-81	21	287	2.42
pMTG/LOTC	Tools	Left mFUG	-30	-63	-21	234	3.19
pMTG/LOTC	Tools	Right mFUG	30	69	21	41	1.95
pMTG/LOTC	Hands	Right STS	57	-48	9	182	2.82
IPL/aIPS	Tools	Left mFUG	-24	-51	-24	65	2.77
IPL/aIPS	Hands	Left postcentral gyrus	-36	-36	66	77	2.25
IPL/aIPS	Hands	Left STS	-39	-54	12	52	1.94

LOTC – lateral occipital temporal cortex; pMTG – posterior middle temporal gyrus; IPL – inferior parietal lobule; aIPS – anterior intraparietal sulcus; mFUG – middle fusiform Gyrus; STS – superior temporal sulcus.

Figure 3A. Whole-brain searchlight correlation between category-preferences and functional connectivity to IPL/aIPS (surface maps).

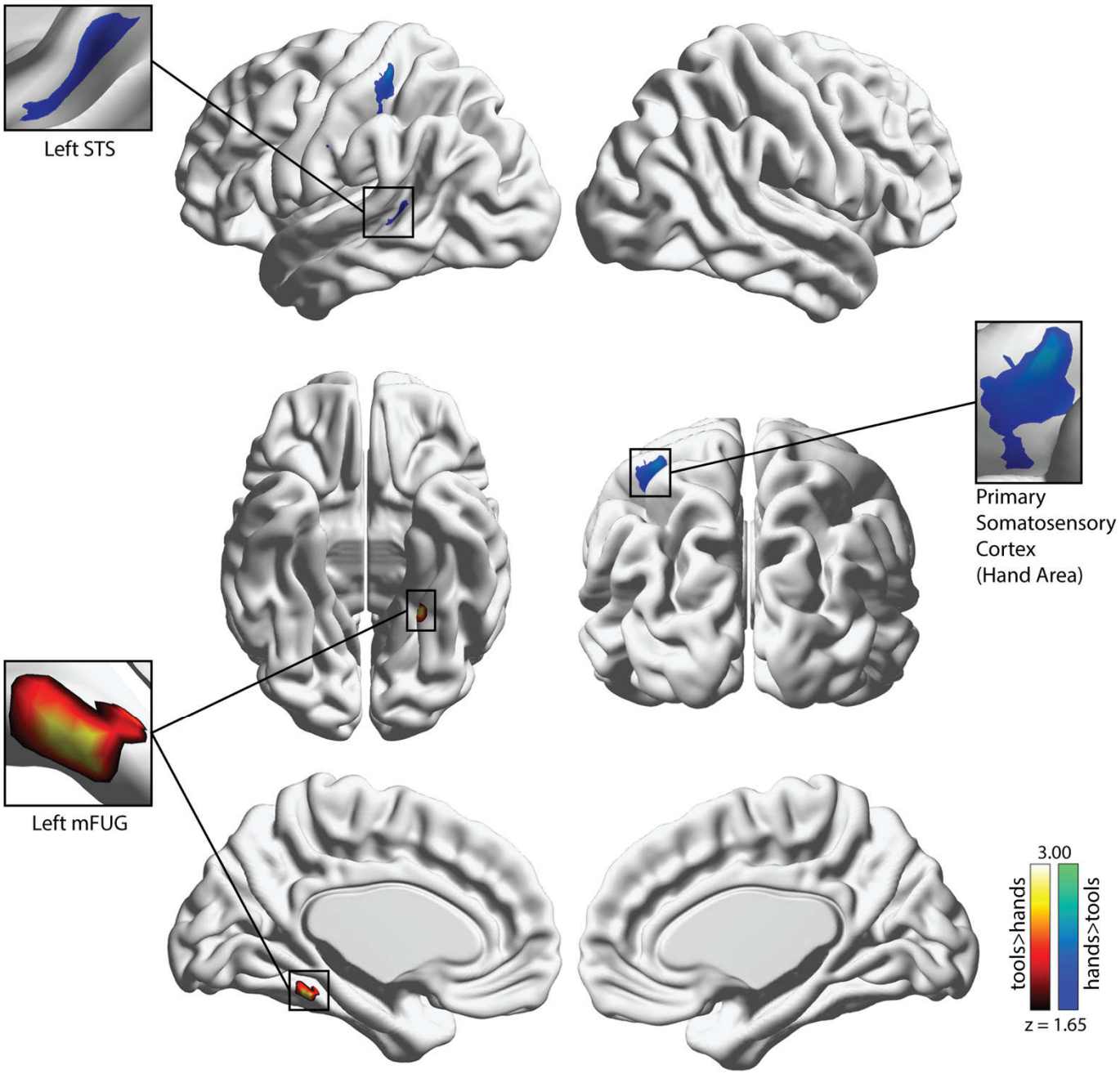

Figure 3B. Whole-brain searchlight correlation between category-preferences and functional connectivity to pMTG/LOTC (surface maps).

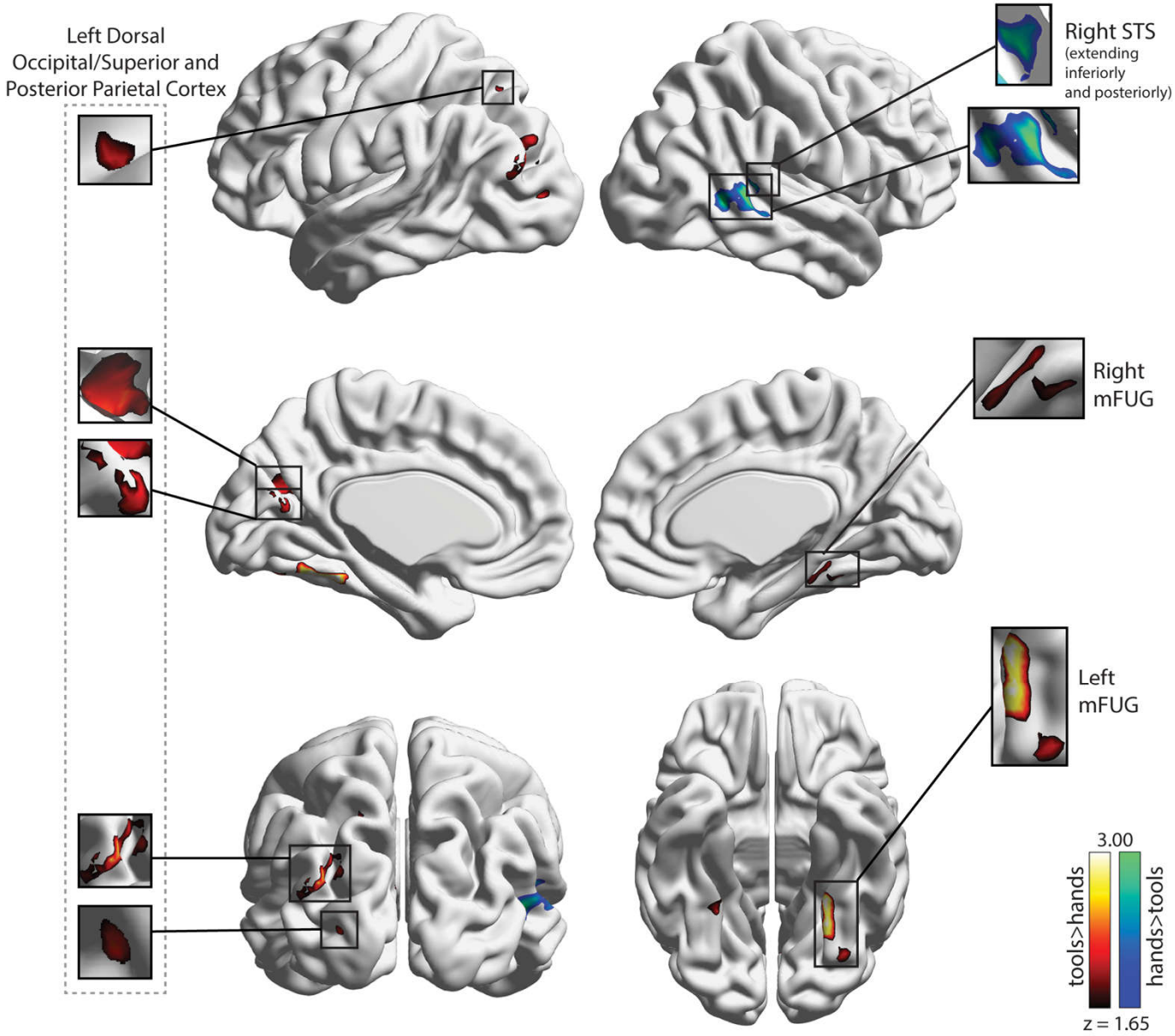

Whole-brain searchlight correlation between category-preferences and functional connectivity (surface maps). (**A**) warm colors indicate higher voxel-wise correlations between tool-preferences and functional connectivity to IPL/aIPS (compared to hand-preferences). Cold colors indicate higher voxel-wise correlations between hand-preferences and functional connectivity to IPL/aIPS (compared to tool-preferences). **(B)** warm colors indicate higher voxel-

wise correlations between tool-preferences and functional connectivity to pMTG/LOTC (compared to hand-preferences). Cold colors indicate higher voxelwise correlations between hand-preferences and functional connectivity to pMTG/LOTC (compared to tool-preferences). All z-maps were corrected for multiple comparisons using TFCE Monte Carlo simulation with 10,000 iterations (Oosterhof et al., 2016).

Discussion

Here we set out to test the hypothesis that local representations relate to distal representations in a category specific way – suggesting that local computations are modulated by local constraints, bottom-up and top-down connections, as well as representations that are distally processed within a category-specific network (Chen et al., 2017; Lee et al., 2019; Mahon & Caramazza, 2011). We did so by looking at regions that are engaged by two different categories – hands and tools – and tested whether functional connectivity from these overlap areas (the tool- and hand-preferring left IPL and left pMTG/LOTC) relate to category-preferences in other distal regions (in this case category-preferring regions in the VTC) in a category-specific way (i.e., differently for hands and tools). That is, we looked at whether functional connections of regions that belong to more than one functionally specified network (in our case the networks that prefer tools and that prefer hands) related to the local processing within distal areas in a category-specific way, disentangling these networks.

Firstly, we focused on VTC and showed that functional connectivity from IPL/aIPS and pMTG/LOTC to tool-preferring mFUG correlated more with tool-preferences than hand-preferences, while functional connectivity from IPL/aIPS and pMTG/LOTC to body-preferring FBA correlated more with hand-preferences than tool-preferences. This suggests that despite the processing overlap for tools and hands in IPL/aIPS and pMTG/LOTC, the functional connections of these regions maintain object

topography by allowing for a category-specific flow of information that is pertinent to computing category-specific representations. This is especially important because VTC has been widely implicated in object recognition, and consistently shows a mosaic of regions engaged by different object categories (e.g., Moshe Bar & Aminoff, 2003; Bracci et al., 2012, 2016; Chao et al., 1999; Chao & Martin, 2000; Downing et al., 2001; Epstein & Kanwisher, 1998; Fox et al., 2009; Kanwisher et al., 1997; Kristensen et al., 2016; Lee et al., 2019; Mahon et al., 2007; Martin et al., 1996; Peelen & Downing, 2007; Perani et al., 1995). This mosaic is related with (and may potentially be dependent on) the information flow from distal regions that belong to the network that is dedicated to the processing of the target network.

Secondly, we explored whether and how this relationship between functional connectivity from our two seed "distal" regions and local category preferences across the whole-brain was present – that is, whether and how the overlap regions allowed for disentangling parts of the tool and hand network across the brain. In our searchlight analysis, we showed that left IPL/aIPS and left pMTG/LOTC correlated with local category preferences in different regions across the brain for the two categories. Specifically, connectivity from pMTG/LOTC was correlated with tool-preferences in a large part of left dorsal occipital cortex, including the superior parietal lobule, and in the mFUG bilaterally, whereas connectivity from IPL/aIPS was correlated with tool-preferences in left mFUG. In what concerns hand representations, connectivity from pMTG/LOTC was correlated with hand-preferences in the right STS, whereas connectivity from IPL/aIPS was correlated with hand-preferences in the left postcentral gyrus and the left STS.

Our data therefore shows that these long-range distal connections function in a category-dependent fashion irrespective of whether the remote region is engaged by

different (but specific) categories. On the one hand, we show that (local) tool representations are associated with computations happening distally within the tool network – the "local" regions that emerged from both of our analyses are clearly part of the tool network (e.g., Almeida et al., 2010; Garcea & Mahon, 2014; Mahon et al., 2007). In fact, using neurostimulation we have shown before that interfering with processing within one node of the tool network will cascade down to the full network (Ruttorf et al., 2019). On the other hand, we show that regions emerging from our analyses for hand representations are part of the hand network and are related to multisensory and movement-sensitive processing (e.g., STS and postcentral gyrus/somatosensory hand area; Beauchamp et al., 2008; Macaluso, 2006).

Furthermore, our data points to representational differences in the kinds distal relationships observed for these two overlap regions. For tool processing, the results obtained for pMTG/LOTC may suggest that this region connects posterior parietal and dorsal occipital regions working on aspects of volumetric analysis of graspable objects such as elongation and grasping status (i.e., is this object graspable; Almeida et al., 2008, 2010, 2014; Fabbri et al., 2016; Fang & He, 2005), with aspects of tool representations in mFUG, potentially related with shape, material, and surface properties (Cant et al., 2009; Cant & Goodale, 2007). On the other hand, IPL and aIPS seem focused exclusively on the left mFUG, a result that seems in line with previous literature showing a preferred relationship between IPL and left mFUG for tool processing (Almeida et al., 2013; Garcea & Mahon, 2014; Kristensen et al., 2016; Lee et al., 2019; Mahon et al., 2013), and potentially related to the passage of information pertinent to object manipulation and functional grasps (e.g., Almeida et al., 2013; Kristensen et al., 2016; Mahon et al., 2013; Valyear and Culham, 2010).

Interestingly, IPL has been heavily associated with acessing function-specific object manipulations (Boronat et al., 2005; Ishibashi et al., 2011; Kellenbach et al., 2003; Mahon et al., 2007) and patients with lesions to IPL present with ideomotor apraxia (i.e., an inability to manipulate everyday objects; Almeida et al., 2018; Buxbaum, Giovannetti, et al., 2000; Buxbaum, Veramonti, et al., 2000; Garcea et al., 2013; Mahon et al., 2007; Ochipa et al., 1994), whereas aIPS is known to be strongly involved in the computation of hand-shapes for object grasping (Binkofski et al., 1999; Binkofski et al., 1998; Culham et al., 2003; Monaco et al., 2011), and in particular in shaping the hand for functional grasps (i.e., grasps that are specific for the manipulation programs necessary to use an object; e.g., Buchwald et al., 2018). This passage of information to IPL and aIPS from ventral temporal cortex may reflect the necessary passage of semantic and functional information that allows for accessing praxis and selecting associated functional grasps (Almeida et al., 2013; Chen et al., 2017; Garcea et al., 2016, 2019; Kristensen et al., 2016).

For hand processing, the difference in the pattern of distal relationships relayed by IPL/aIPS and pMTG/LOTC may be related to either more motor or more social aspects pertinent to the computations being performed locally. On the one hand, IPL/aIPS is distally related with regions that are purportedly implicated in motor planning and execution such as the left STS (Liebenthal et al., 2014; Rizzolatti et al., 1996) and postcentral gyrus – an area well known for being the location of the primary somatosensory cortex (Penfield & Boldrey, 1937), but also involved in grasp action (Castiello, 2005; Iwamura & Tanaka, 1996). More specifically, connectivity with postcentral gyrus/somatosensory cortex was restricted to a location involved in somatosensory processing for hands (Horovitz et al., 2013; Lavrysen et al., 2012). On the

other hand, distal relationships associated with pMTG/LOTC were found within the right STS – a region that has been implicated in aspects of social cognition and face and body expression (Bonda et al., 1996; Narumoto et al., 2001; Puce et al., 1998; for a review see Puce & Perrett, 2003) and also implicated in the imitation of observed actions (Iacoboni et al., 2001).

Note that there are some differences in results between our *a priori* category-specific ROIs and our whole-brain searchlight analysis, specifically in what concerns the lack of an effect in FBA under the searchlight approach. This could be due to differences in the two analytical pipelines – namely that in the ROI analysis we use a more focused theoretically based approach, whereas in the searchlight we are less theory-driven and have to account for a much larger number of comparison by using stringent corrections. It may also mean, however, that while for tool items, the medial aspects of the fusiform gyrus are truly central for the passage of information within the network, the same may not be true for hand stimuli in terms of the FBA – perhaps motor and social information, aspects that seem to be central in governing hand processing, are not central drivers of the computations happening within FBA. Nevertheless, and albeit not so prominently, the information within FBA may still flow within the hand network.

Our study has some caveats that could not be fully taken care of. Although functional connectivity and stimulus preferences were computed over entirely independent datasets, so there was no circularity when selecting datasets (Kriegeskorte et al., 2009), we cannot infer causality concerning how these connectivity constraints are imposed. Nevertheless, and because our results are robust, we believe that we should obtain similar results if a causal approach was to be followed as we have done before (Lee et al., 2019; Ruttorf et al., 2019) – i.e., if we were to use non-invasive neurostimulation within these areas of overlap, we should see category-specific effects in the parts of the

brain implicated in the current study (e.g., the dorsal occipital cortex for tool-preferences and their correlation with functional connectivity from IPL/aIPS). Finally, we should also note that our study may have reduced power given our limited sample size.

In conclusion, our results show how areas that purportedly respond equally to two different categories (that of tools and hands) present different patterns of connections for their preferred categories. This suggests that the same neurons (or at least neurons within the same voxels) in such areas process and send category pertinent information to particular category-specific networks in a way that is dependent on the stimuli being processed. That is, distal connections from an overlap area are dependent on the category being processed at a particular time point, perhaps changing representations and computations, while attributing connectivity a crucial role in determining object representation.

References

Almeida, J., Amaral, L., Garcea, F. E., Aguiar de Sousa, D., Xu, S., Mahon, B. Z., & Martins, I. P. (2018). Visual and visuomotor processing of hands and tools as a case study of cross talk between the dorsal and ventral streams. *Cognitive Neuropsychology*, *35*(5–6), 288–303. https://doi.org/10.1080/02643294.2018.1463980

Almeida, J., Fintzi, A. R., & Mahon, B. Z. (2013). Tool manipulation knowledge is retrieved by way of the ventral visual object processing pathway. *Cortex*, *49*(9), 2334–2344. https://doi.org/10.1016/j.cortex.2013.05.004

Almeida, J., Mahon, B. Z., & Caramazza, A. (2010). The role of the dorsal visual processing stream in tool identification. *Psychological Science : A Journal of the American Psychological Society / APS*, *21*(6), 772–778. https://doi.org/10.1177/0956797610371343

Almeida, J., Mahon, B. Z., Nakayama, K., & Caramazza, A. (2008). Unconscious processing dissociates along categorical lines. *Proceedings of the National Academy of Sciences of the United States of America*, *105*(39), 15214–15218. https://doi.org/10.1073/pnas.0805867105

Almeida, J., Mahon, B. Z., Zapater-Raberov, V., Dziuba, A., Cabaço, T., Marques, J. F., & Caramazza, A. (2014). Grasping with the eyes: The role of elongation in visual recognition of manipulable objects. *Cognitive, Affective and Behavioral Neuroscience*, *14*(1), 319–335. https://doi.org/10.3758/s13415-013-0208-0

Almeida, J., Martins, A. R., Bergström, F., Amaral, L., Freixo, A., Ganho-Ávila, A., Kristensen, S., Lee, D., Nogueira, J., & Ruttorf, M. (2017). Polarity-specific transcranial Direct Current Stimulation effects on object-selective neural responses

in the Inferior Parietal Lobe. *Cortex*, *4*, 6–11. https://doi.org/10.1016/j.cortex.2017.07.001

Ashburner, J. (2007). A fast diffeomorphic image registration algorithm. *NeuroImage*, *38*(1), 95–113. https://doi.org/10.1016/j.neuroimage.2007.07.007

Bar, M., Kassam, K. S., Ghuman, A. S., Boshyan, J., Schmidt, A. M., Dale, A. M., Hämäläinen, M. S., Marinkovic, K., Schacter, D. L., Rosen, B. R., & Halgren, E. (2006). Top-down facilitation of visual recognition. *Proceedings of the National Academy of Sciences of the United States of America*, *103*(2), 449–454. https://doi.org/10.1073/pnas.0507062103

Bar, Moshe, & Aminoff, E. (2003). Cortical analysis of visual context. *Neuron*, *38*(2), 347–358. https://doi.org/10.1016/S0896-6273(03)00167-3

Beauchamp, M. S., Yasar, N. E., Frye, R. E., & Ro, T. (2008). Touch, sound and vision in human superior temporal sulcus. *NeuroImage*, *41*(3), 1011–1020. https://doi.org/10.1016/j.neuroimage.2008.03.015

Binkofski, F., Buccino, G., Posse, S., Seitz, R. J., Rizzolatti, G., & Freund, H.-J. (1999). A fronto-parietal circuit for object manipulation in man: evidence from an fMRI-study. *European Journal of Neuroscience*, *11*(9), 3276–3286. https://doi.org/10.1046/j.1460-9568.1999.00753.x

Binkofski, Ferdinand, Dohle, C., Posse, S., Stephan, K. M., Hefter, H., Seitz, R. J., & Freund, H. J. (1998). Human anterior intraparietal area subserves prehension: A combined lesion and functional MRI activation study. *Neurology*, *50*(5), 1253–1259. https://doi.org/10.1212/WNL.50.5.1253

Bonda, E., Petrides, M., Ostry, D., & Evans, A. (1996). Specific involvement of human parietal systems and the amygdala in the perception of biological motion. *Journal of Neuroscience*, *16*(11), 3737–3744. https://doi.org/10.1523/jneurosci.16-11-

03737.1996

Boronat, C. B., Buxbaum, L. J., Coslett, H. B., Tang, K., Saffran, E. M., Kimberg, D. Y., & Detre, J. A. (2005). Distinctions between manipulation and function knowledge of objects: Evidence from functional magnetic resonance imaging. *Cognitive Brain Research*, *23*(2–3), 361–373. https://doi.org/10.1016/j.cogbrainres.2004.11.001

Bracci, S., Cavina-Pratesi, C., Connolly, J. D., & Ietswaart, M. (2016). Representational content of occipitotemporal and parietal tool areas. *Neuropsychologia*, *84*, 81–88. https://doi.org/10.1016/j.neuropsychologia.2015.09.001

Bracci, S., Cavina-Pratesi, C., Ietswaart, M., Caramazza, A., & Peelen, M. V. (2012). Closely overlapping responses to tools and hands in left lateral occipitotemporal cortex. *Journal of Neurophysiology*, *107*(5), 1443–1446. https://doi.org/10.1152/jn.00619.2011

Bracci, S., Ietswaart, M., Peelen, M. V., & Cavina-Pratesi, C. (2010). Dissociable neural responses to hands and non-hand body parts in human left extrastriate visual cortex. *Journal of Neurophysiology*, *103*(6), 3389–3397. https://doi.org/10.1152/jn.00215.2010

Bracci, S., & Peelen, M. V. (2013). Body and object effectors: The organization of object representations in high-level visual cortex reflects body-object interactions. *Journal of Neuroscience*, *33*(46), 18247–18258. https://doi.org/10.1523/JNEUROSCI.1322-13.2013

Buchwald, M., Przybylski, Ł., & Króliczak, G. (2018). Decoding Brain States for Planning Functional Grasps of Tools: A Functional Magnetic Resonance Imaging Multivoxel Pattern Analysis Study. *Journal of the International Neuropsychological Society*, *24*, 1013–1025.

https://doi.org/10.1017/S1355617718000590

Buffalo, E. A., Fries, P., Landman, R., Liang, H., & Desimone, R. (2010). A backward progression of attentional effects in the ventral stream. *Proceedings of the National Academy of Sciences of the United States of America*, *107*(1), 361–365. https://doi.org/10.1073/pnas.0907658106

Buxbaum, L. J., Giovannetti, T., & Libon, D. (2000). The role of the dynamic body schema in praxis: Evidence from primary progressive apraxia. *Brain and Cognition*, *44*(2), 166–191. https://doi.org/10.1006/brcg.2000.1227

Buxbaum, L. J., Veramonti, T., & Schwartz, M. F. (2000). Function and manipulation tool knowledge in apraxia: Knowing "What For" but not "How." *Neurocase*, *6*(2), 83–97. https://doi.org/10.1080/13554790008402763

Cant, J. S., Arnott, S. R., & Goodale, M. A. (2009). fMR-adaptation reveals separate processing regions for the perception of form and texture in the human ventral stream. *Experimental Brain Research*, *192*(3), 391–405. https://doi.org/10.1007/s00221-008-1573-8

Cant, J. S., & Goodale, M. A. (2007). Attention to form or surface properties modulates different regions of human occipitotemporal cortex. *Cerebral Cortex (New York, N.Y. : 1991)*, *17*(3), 713–731. https://doi.org/10.1093/cercor/bhk022

Caramazza, A., & Shelton, J. R. (1998). *Domain-Speci[a]c Knowledge Systems in the Brain: The Animate-Inanimate Distinction*.

Caspers, S., Geyer, S., Schleicher, A., Mohlberg, H., Amunts, K., & Zilles, K. (2006). The human inferior parietal cortex: Cytoarchitectonic parcellation and interindividual variability. *NeuroImage*, *33*(2), 430–448. https://doi.org/10.1016/j.neuroimage.2006.06.054

Castiello, U. (2005). The neuroscience of grasping. *Nature Reviews Neuroscience*, *6*(9),

726–736. https://doi.org/10.1038/nrn1744

Chao, L. L., Haxby, J. V., & Martin, A. (1999). Attribute-based neural substrates in temporal cortex for perceiving and knowing about objects. *Nature Neuroscience*, *2*(10), 913–919. https://doi.org/10.1038/13217

Chao, L. L., & Martin, A. (2000). Representation of manipulable man-made objects in the dorsal stream. *NeuroImage*, *12*(4), 478–484. https://doi.org/10.1006/nimg.2000.0635

Chen, Q., Garcea, F. E., Almeida, J., & Mahon, B. Z. (2017). Connectivity-based constraints on category-specificity in the ventral object processing pathway. *Neuropsychologia*, *105*(July), 184–196. https://doi.org/10.1016/j.neuropsychologia.2016.11.014

Choi, H. J., Zilles, K., Mohlberg, H., Schleicher, A., Fink, G. R., Armstrong, E., & Amunts, K. (2006). Cytoarchitectonic identification and probabilistic mapping of two distinct areas within the anterior ventral bank of the human intraparietal sulcus. *Journal of Comparative Neurology*, *495*(1), 53–69. https://doi.org/10.1002/cne.20849

Culham, J. C., Danckert, S. L., DeSouza, J. F. X., Gati, J. S., Menon, R. S., & Goodale, M. A. (2003). Visually guided grasping produces fMRI activation in dorsal but not ventral stream brain areas. *Experimental Brain Research*, *153*(2), 180–189. https://doi.org/10.1007/s00221-003-1591-5

Downing, P. E., Jiang, Y., Shuman, M., & Kanwisher, N. (2001). A cortical area selective for visual processing of the human body. *Science (New York, N.Y.)*, *293*(5539), 2470–2473. https://doi.org/10.1126/science.1063414

Epstein, R., & Kanwisher, N. (1998). A cortical representation of the local visual environment. *Nature*, *392*(6676), 598–601. https://doi.org/10.1038/33402

Fabbri, S., Stubbs, K. M., Cusack, R., & Culham, J. C. (2016). Disentangling representations of object and grasp properties in the human brain. *Journal of Neuroscience*, *36*(29), 7648–7662. https://doi.org/10.1523/JNEUROSCI.0313-16.2016

Fang, F., & He, S. (2005). Cortical responses to invisible objects in the human dorsal and ventral pathways. *Nature Neuroscience*, *8*(10), 1380–1385. https://doi.org/10.1038/nn1537

Fintzi, A. R., & Mahon, B. Z. (2014). A bimodal tuning curve for spatial frequency across left and right human orbital frontal cortex during object recognition. *Cerebral Cortex (New York, N.Y. : 1991)*, *24*(5), 1311–1318. https://doi.org/10.1093/cercor/bhs419

Fox, C. J., Iaria, G., & Barton, J. J. S. (2009). Defining the face processing network: Optimization of the functional localizer in fMRI. *Human Brain Mapping*, *30*(5), 1637–1651. https://doi.org/10.1002/hbm.20630

Freud, E., Culham, J. C., Plaut, D. C., & Behrmann, M. (2017). The large-scale organization of shape processing in the ventral and dorsal pathways. *ELife*, *6*. https://doi.org/10.7554/eLife.27576

Garcea, F. E., Almeida, J., Sims, M. H., Nunno, A., Meyers, S. P., Li, Y. M., Walter, K., Pilcher, W. H., & Mahon, B. Z. (2019). Domain-Specific Diaschisis: Lesions to Parietal Action Areas Modulate Neural Responses to Tools in the Ventral Stream. *Cerebral Cortex*, 3168–3181. https://doi.org/10.1093/cercor/bhy183

Garcea, F. E., Dombovy, M., & Mahon, B. Z. (2013). Preserved Tool Knowledge in the Context of Impaired Action Knowledge: Implications for Models of Semantic Memory. *Frontiers in Human Neuroscience*, *7*(MAR), 120. https://doi.org/10.3389/fnhum.2013.00120

Garcea, F. E., Kristensen, S., Almeida, J., & Mahon, B. Z. (2016). Resilience to the contralateral visual field bias as a window into object representations. *Cortex*, *81*, 14–23. https://doi.org/10.1016/j.cortex.2016.04.006

Garcea, F. E., & Mahon, B. Z. (2014). Parcellation of left parietal tool representations by functional connectivity. *Neuropsychologia*, *60*(1), 131–143. https://doi.org/10.1016/j.neuropsychologia.2014.05.018

Grill-Spector, K., & Malach, R. (2004). the Human Visual Cortex. *Annual Review of Neuroscience*, *27*(1), 649–677. https://doi.org/10.1146/annurev.neuro.27.070203.144220

Grosbras, M. H., & Paus, T. (2006). Brain networks involved in viewing angry hands or faces. *Cerebral Cortex*, *16*(8), 1087–1096. https://doi.org/10.1093/cercor/bhj050

Haxby, J. V., Gobbini, M. I., Furey, M. L., Ishai, A., Schouten, J. L., & Pietrini, P. (2001). Distributed and overlapping representations of faces and objects in ventral temporal cortex. *Science*, *293*(5539), 2425–2430. https://doi.org/10.1126/science.1063736

Holm, S. (1978). Board of the Foundation of the Scandinavian Journal of Statistics A Simple Sequentially Rejective Multiple Test Procedure Author (s): Sture Holm Published by : Wiley on behalf of Board of the Foundation of the Scandinavian Journal of Statistics Stable U. *Scandinavian Journal of Statistics*, *6*(2), 65–70.

Horovitz, S. G., Gallea, C., Najee-ullah, M. A., & Hallett, M. (2013). Functional Anatomy of Writing with the Dominant Hand. *PLoS ONE*, *8*(7). https://doi.org/10.1371/journal.pone.0067931

Hutchison, R. M., Culham, J. C., Everling, S., Flanagan, J. R., & Gallivan, J. P. (2014). Distinct and distributed functional connectivity patterns across cortex reflect the domain-specific constraints of object, face, scene, body, and tool category-

selective modules in the ventral visual pathway. *NeuroImage*, *96*, 216–236. https://doi.org/10.1016/j.neuroimage.2014.03.068

Hutchison, R. M., & Gallivan, J. P. (2018). Functional coupling between frontoparietal and occipitotemporal pathways during action and perception. *Cortex*, *98*, 8–27. https://doi.org/10.1016/j.cortex.2016.10.020

Iacoboni, M., Koski, L. M., Brass, M., Bekkering, H., Woods, R. P., Dubeau, M. C., Mazziotta, J. C., & Rizzolatti, G. (2001). Reafferent copies of imitated actions in the right superior temporal cortex. *Proceedings of the National Academy of Sciences of the United States of America*, *98*(24), 13995–13999. https://doi.org/10.1073/pnas.241474598

Ishibashi, R., Lambon Ralph, M. A., Saito, S., & Pobric, G. (2011). Different roles of lateral anterior temporal lobe and inferior parietal lobule in coding function and manipulation tool knowledge: Evidence from an rTMS study. *Neuropsychologia*, *49*(5), 1128–1135. https://doi.org/10.1016/j.neuropsychologia.2011.01.004

Iwamura, Y., & Tanaka, M. (1996). Representation of reaching and grasping in the monkey postcentral gyrus. *Neuroscience Letters*, *214*(2–3), 147–150. https://doi.org/10.1016/0304-3940(96)12911-6

Kamarov, O. (2020). *Heteroskedasticity test - File Exchange - MATLAB Central*. https://www.mathworks.com/matlabcentral/fileexchange/24722-heteroskedasticity-test

Kanwisher, N., McDermott, J., & Chun, M. M. (1997). The fusiform face area: a module in human extrastriate cortex specialized for face perception. *The Journal of Neuroscience : The Official Journal of the Society for Neuroscience*, *17*(11), 4302–4311. https://doi.org/10.1098/Rstb.2006.1934

Kellenbach, M. L., Brett, M., & Patterson, K. (2003). Actions speak louder than

functions: The importance of manipulability and action in tool representation. *Journal of Cognitive Neuroscience*, *15*(1), 30–46. https://doi.org/10.1162/089892903321107800

Konkle, T., & Caramazza, A. (2013). Tripartite organization of the ventral stream by animacy and object size. *Journal of Neuroscience*, *33*(25), 10235–10242. https://doi.org/10.1523/JNEUROSCI.0983-13.2013

Kreiman, G., Serre, T., & Poggio, T. (2010). On the limits of feed-forward processing in visual object recognition. *Journal of Vision*, *7*(9), 1041–1041. https://doi.org/10.1167/7.9.1041

Kriegeskorte, N., Goebel, R., & Bandettini, P. (2006). Information-based functional brain mapping. *Proceedings of the National Academy of Sciences of the United States of America*, *103*(10), 3863–3868. https://doi.org/10.1073/pnas.0600244103

Kriegeskorte, N., Mur, M., Ruff, D. A., Kiani, R., Bodurka, J., Esteky, H., Tanaka, K., & Bandettini, P. A. (2008). Matching Categorical Object Representations in Inferior Temporal Cortex of Man and Monkey. *Neuron*, *60*(6), 1126–1141. https://doi.org/10.1016/j.neuron.2008.10.043

Kriegeskorte, N., Simmons, W. K., Bellgowan, P. S., & Baker, C. I. (2009). Circular analysis in systems neuroscience: The dangers of double dipping. *Nature Neuroscience*, *12*(5), 535–540. https://doi.org/10.1038/nn.2303

Kristensen, S., Garcea, F. E., Mahon, B. Z., & Almeida, J. (2016). Temporal frequency tuning reveals interactions between the dorsal and ventral visual streams. *Journal of Cognitive Neuroscience*, *28*(9), 1295–1302. https://doi.org/10.1162/jocn_a_00969

Lavrysen, A., Heremans, E., Peeters, R., Wenderoth, N., Feys, P., Swinnen, S. P., & Helsen, W. F. (2012). Hemispheric asymmetries in goal-directed hand movements

are independent of hand preference. *NeuroImage*, *62*(3), 1815–1824. https://doi.org/10.1016/j.neuroimage.2012.05.033

Lee, D., Mahon, B. Z., & Almeida, J. (2019). Action at a distance on object-related ventral temporal representations. *Cortex*, *117*, 157–167. https://doi.org/10.1016/j.cortex.2019.02.018

Levy, I., Hasson, U., Avidan, G., Hendler, T., & Malach, R. (2001). *Center-periphery organization of human object areas*. http://neurosci.nature.com

Liebenthal, E., Desai, R. H., Humphries, C., Sabri, M., & Desai, A. (2014). The functional organization of the left STS: a large scale meta-analysis of PET and fMRI studies of healthy adults. *Frontiers in Neuroscience*, *8*(SEP), 289. https://doi.org/10.3389/fnins.2014.00289

Macaluso, E. (2006). Multisensory Processing in Sensory-Specific Cortical Areas. *The Neuroscientist*, *12*(4), 327–338. https://doi.org/10.1177/1073858406287908

Mahon, B. Z., Anzellotti, S., Schwarzbach, J., Zampini, M., & Caramazza, A. (2009). Category-Specific Organization in the Human Brain Does Not Require Visual Experience. *Neuron*, *63*(3), 397–405. https://doi.org/10.1016/j.neuron.2009.07.012

Mahon, B. Z., & Caramazza, A. (2009). Concepts and Categories: A Cognitive Neuropsychological Perspective. *Annual Review of Psychology*, *60*(1), 27–51. https://doi.org/10.1146/annurev.psych.60.110707.163532

Mahon, B. Z., & Caramazza, A. (2011). What drives the organization of object knowledge in the brain? *Trends in Cognitive Sciences*, *15*(3), 97–103. https://doi.org/10.1016/j.tics.2011.01.004

Mahon, B. Z., Kumar, N., & Almeida, J. (2013). Spatial frequency tuning reveals interactions between the dorsal and ventral visual systems. *Journal of Cognitive Neuroscience*, *25*(6), 862–871. https://doi.org/10.1162/jocn_a_00370

Mahon, B. Z., Milleville, S. C., Negri, G. A. L., Rumiati, R. I., Caramazza, A., & Martin, A. (2007). Action-Related Properties Shape Object Representations in the Ventral Stream. *Neuron*, *55*(3), 507–520. https://doi.org/10.1016/j.neuron.2007.07.011

Martin, A., Wiggs, C. L., Ungerleider, L. G., & Haxby, J. V. (1996). Neural correlates of category-specific knowledge. *Nature*, *379*(6566), 649–652. https://doi.org/10.1038/379649a0

Meier, J. D., Aflalo, T. N., Kastner, S., & Graziano, M. S. A. (2008). Complex organization of human primary motor cortex: A high-resolution fMRI study. *Journal of Neurophysiology*, *100*(4), 1800–1812. https://doi.org/10.1152/jn.90531.2008

Monaco, S., Cavina-Pratesi, C., Sedda, A., Fattori, P., Galletti, C., & Culham, J. C. (2011). Functional magnetic resonance adaptation reveals the involvement of the dorsomedial stream in hand orientation for grasping. *Journal of Neurophysiology*, *106*(5), 2248–2263. https://doi.org/10.1152/jn.01069.2010

Narumoto, J., Okada, T., Sadato, N., Fukui, K., & Yonekura, Y. (2001). Attention to emotion modulates fMRI activity in human right superior temporal sulcus. *Cognitive Brain Research*, *12*(2), 225–231. https://doi.org/10.1016/S0926-6410(01)00053-2

Noppeney, U., Price, C. J., Penny, W. D., & Friston, K. J. (2006). Two distinct neural mechanisms for category-selective responses. *Cerebral Cortex (New York, N.Y. : 1991)*, *16*(3), 437–445. https://doi.org/10.1093/cercor/bhi123

Norman-Haignere, S. V., McCarthy, G., Chun, M. M., & Turk-Browne, N. B. (2012). Category-selective background connectivity in ventral visual cortex. *Cerebral Cortex*, *22*(2), 391–402. https://doi.org/10.1093/cercor/bhr118

Ochipa, C., Rothi, L. J. G., & Heilman, K. M. (1994). Conduction apraxia. *Journal of Neurology, Neurosurgery and Psychiatry*, *57*(10), 1241–1244. https://doi.org/10.1136/jnnp.57.10.1241

Oosterhof, N. N., Connolly, A. C., & Haxby, J. V. (2016). CoSMoMVPA: Multi-Modal Multivariate Pattern Analysis of Neuroimaging Data in Matlab/GNU Octave. *Frontiers in Neuroinformatics*, *10*(JUL), 27. https://doi.org/10.3389/fninf.2016.00027

Peelen, M. V., & Downing, P. E. (2007). The neural basis of visual body perception. In *Nature Reviews Neuroscience* (Vol. 8, Issue 8, pp. 636–648). Nature Publishing Group. https://doi.org/10.1038/nrn2195

Peeters, R. R., Rizzolatti, G., & Orban, G. A. (2013). Functional properties of the left parietal tool use region. *NeuroImage*, *78*, 83–93. https://doi.org/10.1016/j.neuroimage.2013.04.023

Penfield, W., & Boldrey, E. (1937). Somatic Motor and Sensory Representation in Man. *Brain*, 389–443. https://doi.org/10.1093/brain/60.4.389

Perani, D., Cappa, S. F., Bettinardi, V., Bressi, S., Gorno-Tempini, M., Matarrese, M., & Fazio, F. (1995). Different neural systems for the recognition of animals and man-made tools. *NeuroReport*, *6*(12), 1637–1641. https://doi.org/10.1097/00001756-199508000-00012

Pessoa, L., Japee, S., Sturman, D., & Ungerleider, L. G. (2006). Target visibility and visual awareness modulate amygdala responses to fearful faces. *Cerebral Cortex*, *16*(3), 366–375. https://doi.org/10.1093/cercor/bhi115

Puce, A., Allison, T., Bentin, S., Gore, J. C., & Mccarthy, G. (1998). *Temporal Cortex Activation in Humans Viewing Eye and Mouth Movements*.

Puce, A., & Perrett, D. (2003). *Electrophysiology and brain imaging of biological*

motion. https://doi.org/10.1098/rstb.2002.1221

Rizzolatti, G., Fadiga, L., Matelli, M., Bettinardi, V., Paulesu, E., Perani, D., & Fazio, F. (1996). Localization of grasp representations in humans by PET: 1. Observation versus execution. *Experimental Brain Research*, *111*(2), 246–252. https://doi.org/10.1007/BF00227301

Roux, F., Djidjeli, I., & Durand, J. (2018). Functional architecture of the somatosensory homunculus detected by electrostimulation. *The Journal of Physiology*, *596*(5), 941–956. https://doi.org/10.1113/JP275243@10.1111/(ISSN)1469-7793.EC2018

Ruttorf, M., Kristensen, S., Schad, L. R., & Almeida, J. (2019). Transcranial Direct Current Stimulation Alters Functional Network Structure in Humans: A Graph Theoretical Analysis. *IEEE Transactions on Medical Imaging*, *38*(12), 1–1. https://doi.org/10.1109/tmi.2019.2915206

Saygin, Z. M., Osher, D. E., Norton, E. S., Youssoufian, D. A., Beach, S. D., Feather, J., Gaab, N., Gabrieli, J. D. E., & Kanwisher, N. (2016). Connectivity precedes function in the development of the visual word form area. *Nature Neuroscience*, *19*(9), 1250–1255. https://doi.org/10.1038/nn.4354

Schwarzbach, J. (2011). A simple framework (ASF) for behavioral and neuroimaging experiments based on the psychophysics toolbox for MATLAB. *Behavior Research Methods*, *43*(4), 1194–1201. https://doi.org/10.3758/s13428-011-0106-8

Smith, S. M., & Nichols, T. E. (2009). Threshold-free cluster enhancement: Addressing problems of smoothing, threshold dependence and localisation in cluster inference. *NeuroImage*, *44*(1), 83–98. https://doi.org/10.1016/j.neuroimage.2008.03.061

Tran, S. M., McGregor, K. M., James, G. A., Gopinath, K., Krishnamurthy, V., Krishnamurthy, L. C., & Crosson, B. (2018). Task-residual functional connectivity of language and attention networks. *Brain and Cognition*, *122*, 52–58.

https://doi.org/10.1016/j.bandc.2018.02.003

Valyear, K. F., & Culham, J. C. (2010). Observing learned object-specific functional grasps preferentially activates the ventral stream. *Journal of Cognitive Neuroscience*, *22*(5), 970–984. https://doi.org/10.1162/jocn.2009.21256

Vocks, S., Busch, M., Grönemeyer, D., Schulte, D., Herpertz, S., & Suchan, B. (2010). Differential neuronal responses to the self and others in the extrastriate body area and the fusiform body area. In *Cognitive, Affective and Behavioral Neuroscience* (Vol. 10, Issue 3, pp. 422–429). Springer. https://doi.org/10.3758/CABN.10.3.422

Walbrin, J., & Almeida, J. (2021). High-level representations in human occipito-temporal cortex are indexed by distal connectivity. *bioRxiv* 2021.02.22.432202; doi: https://doi.org/10.1101/2021.02.22.432202.

Whitfield-Gabrieli, S., & Nieto-Castanon, A. (2012). Conn: A Functional Connectivity Toolbox for Correlated and Anticorrelated Brain Networks. *Brain Connectivity*, *2*(3), 125–141. https://doi.org/10.1089/brain.2012.0073

Zhang, H., Tian, J., Liu, J., Li, J., & Lee, K. (2009). Intrinsically organized network for face perception during the resting state. *Neuroscience Letters*, *454*(1), 1–5. https://doi.org/10.1016/j.neulet.2009.02.054

Supplementary Material

Supplementary Figure 1. Location of the individual IPL/aIPS ROIs.

Supplementary Figure 2. Whole-brain searchlight correlation between category-preferences and functional connectivity (volume maps).

Supplementary Figure 3. Location of the right STS cluster from the searchlight in relation to tool and hand right pMTG/LOTC.

Supplementary Table 1. Overlap between each individual IPL/aIPS ROI and: a) the parcellations of the intraparietal sulcus proposed by Choi et al. (2006); b) the parcellations proposed by Caspers et al. (2006) of the left inferior parietal lobule (Supramarginal Gyrus).

Supplementary Figure 1. Location of the individual IPL/aIPS ROIs.

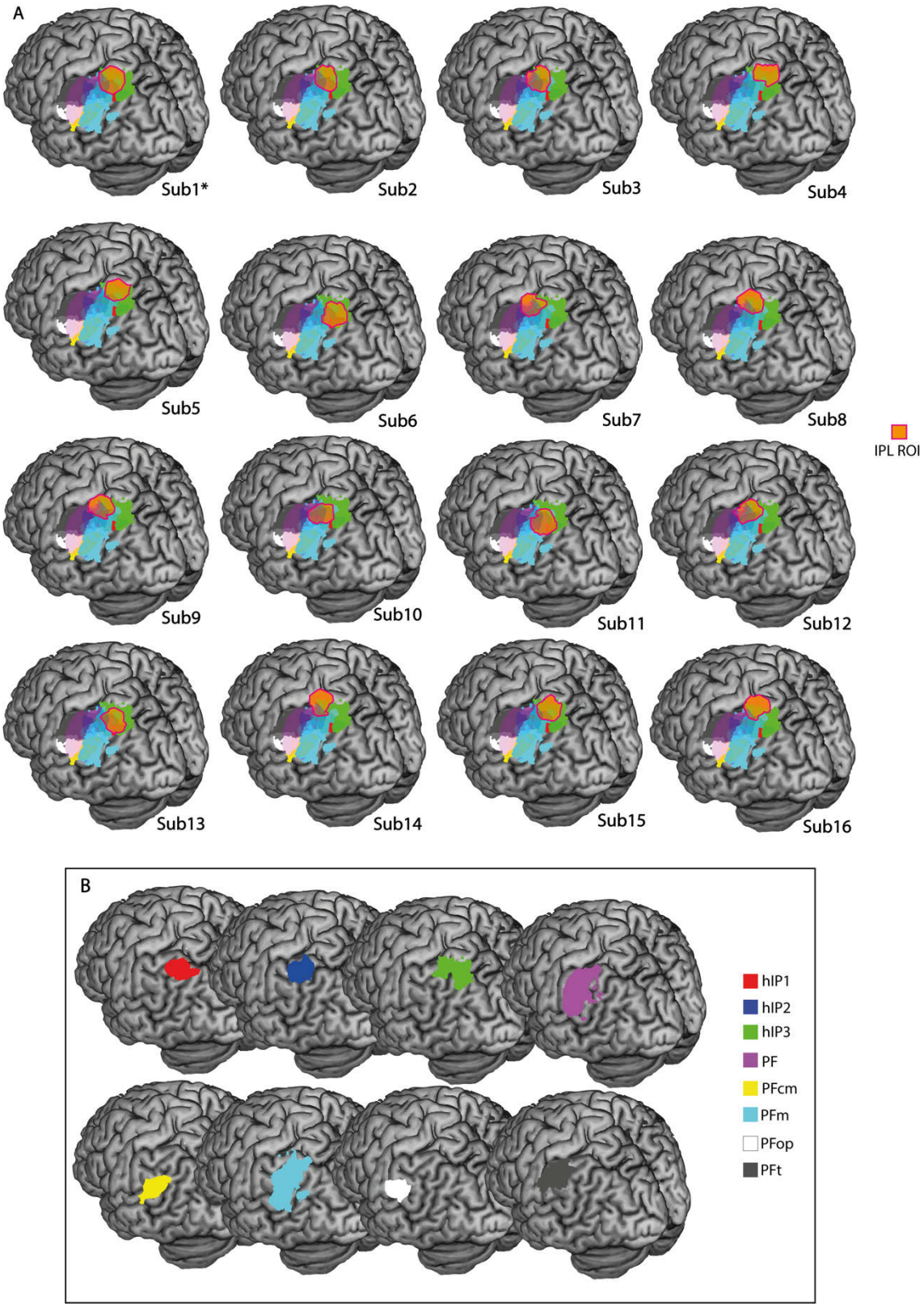

(A) Location of the individual IPL/aIPS ROIs overlapped with the parcellations of the IPL (Supramarginal Gyrus) and intraparietal sulcus. **(B)** The different regions/parcel included in the left IPL (Supramarginal Gyrus) and left intraparietal sulcus as proposed in Caspers et al. (2006) and by Choi et al. (2006). *Because subject 1 did not have enough data to define the individual ROIs, we used the group peak to create them.

Supplementary Figure 2. Whole-brain searchlight correlation between category-preferences and functional connectivity (volume maps).

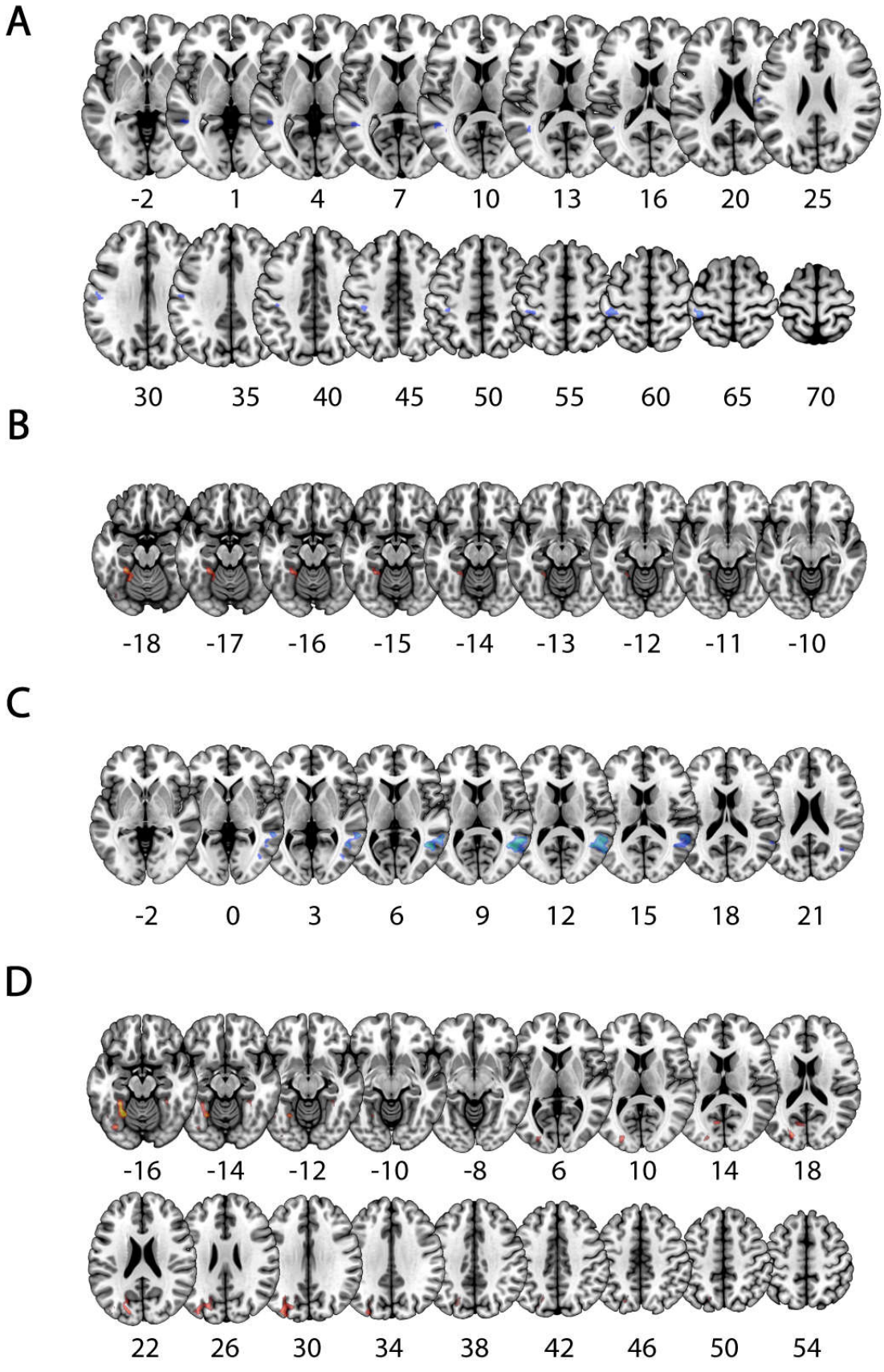

(**A**) cold colors indicate higher voxelwise correlations between hand-preferences and functional connectivity to IPL/aIPS (compared to tool-preferences). (**B**) warm colors indicate higher voxelwise correlations between tool-preferences and functional connectivity to IPL/aIPS (compared to hand-preferences). (**C**) cold colors indicate higher voxelwise correlations between hand-preferences and functional connectivity to pMTG/LOTC (compared to tool-preferences). (**D**) warm colors indicate higher voxelwise correlations between tool-preferences and functional connectivity to pMTG/LOTC (compared to hand-preferences).

Supplementary Figure 3. Location of the right STS cluster from the searchlight in relation to tool and hand right pMTG/LOTC.

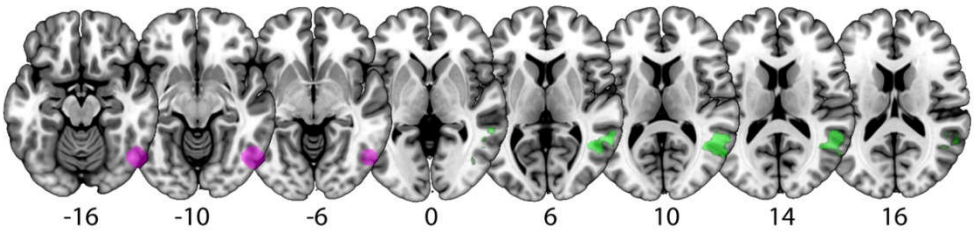

The right STS cluster (green) obtained in the whole-brain searchlight analysis for the correlation between connectivity coming from the left pMTG/LOTC and hand-preferences does not overlap with a functionally defined right pMTG/LOTC hand/tool overlap region (purple).

Supplementary Table 1. Overlap between each individual IPL/aIPS ROI and: a) the parcellations of the intraparietal sulcus proposed by Choi et al. (2006); b) the parcellations proposed by Caspers et al. (2006) of the left inferior parietal lobule (Supramarginal Gyrus).

Overlap between each individual IPL/aIPS ROI and: a) the parcellations of the intraparietal sulcus proposed by Choi et al. (2006); b) the parcellations proposed by Caspers et al. (2006) of the left inferior parietal lobule (Supramarginal Gyrus).

	a) intraparietal sulcus			**b) inferior parietal lobule (Supramarginal Gyrus)**				
	hIP1	**hIP2**	**hIP3**	**PF**	**PFcm**	**PFm**	**PFop**	**Pft**
Sub1	x	x	x	x		x		
Sub2	x	x	x	x		x		
Sub3	x	x	x	x		x		
Sub4	x		x			x		
Sub5	x	x	x			x		
Sub6	x	x	x			x		
Sub7	x	x	x	x		x		x
Sub8	x	x	x	x		x		
Sub9	x	x	x	x		x		
Sub10	x	x	x	x		x		x
Sub11	x	x	x	x				
Sub12	x	x	x	x		x		x
Sub13	x	x	x			x		
Sub14	x	x	x	x		x		
Sub15	x	x	x			x		
Sub16	x	x	x	x		x		